Long-term deformation behaviour of timber columns: Monitoring of a tall timber building in Switzerland

(article starts on next page)

Long-term deformation behaviour of timber columns: Monitoring of a tall timber building in Switzerland

Robert Jockwer [a],[*], Philippe Grönquist [b], Andrea Frangi [b]

[a] *Division of Structural Engineering, Department of Architecture and Civil Engineering (ACE), Chalmers University of Technology, Sven Hultins gata 6, 412 96 Göteborg, Sweden*
[b] *ETH Zurich, Institute of Structural Engineering, Stefano-Franscini-Platz 5, CH-8093 Zürich, Switzerland*

ABSTRACT

Knowledge on the short and long term deformation behavior of highly loaded components in tall timber buildings is important in view of improving future design possibilities with respect to serviceability, both in the construction and in the operational state. In this paper, we present the results of a monitoring case-study on a tall timber-hybrid building in Switzerland, a 15 storey and 60 m high office building completed in 2019. A fibre-optic measuring system showed an increase of the deformation with increasing load during the construction phase of highly stressed spruce-GLT and beech-LVL columns. However, the highest strain values were not reported in the columns themselves but at the ceiling transitions and in the area near their supports. The measurements on the columns were compared with model calculations for long-term deformation of timber elements in order to differentiate single components of the total deformation caused by load, time, and changes in climate during the construction. Over a monitoring period of a year, good agreement of the modelled deformations could be confirmed, which indicates that such models could be well suited for future usage in serviceability design of tall timber buildings.

1. Introduction

Nowadays, a trend towards global increase in construction of tall timber buildings [1] can be observed. This type of construction, enabled by recent developments in both timber manufacturing and engineering, but also general client awareness, offers a competitive alternative in the high-rise building market. This is especially true in terms of its potential of reduction of climate-impacting emissions production as compared to traditional high-rise building structures [2,3]. In Switzerland, with the change of the fire protection regulations [4], timber high-rise buildings with a height of 30 m or above can be built as of January 2015. Recently, Switzerland's first two tall timber buildings have been realized in the municipality of Risch-Rotkreuz in the canton of Zug [5]. The first building, *Suurstoffi S22*, completed in 2018, is an office building with 10 floors above ground and a height of 36 m [6]. The second one, *Arbo* (Fig. 1), completed in 2019, is a 15-storey office building with a height of 60 m. The building *Arbo*, which will constitute the case-study object of deformation monitoring presented in this paper, was realized as a timber-hybrid construction. In fact, global trends in tall timber buildings show that there is a shift towards hybridisation where, as in the building

Arbo, cores are made out of reinforced concrete (RC) [7]. The hybridisation using a RC core targets better structural safety and performance by providing efficient horizontal bracing, which is increasingly important with increasing building height. A prominent and pioneering built example of this type of construction is the 53 m tall *Brock Commons Tallwood House* in Vancouver, Canada [8–10].

In the planning and structural design of timber high-rise buildings, deformations occurring at the structural level are often assessed and evaluated more critically in comparison to steel and solid high-rise buildings. This applies, among others, specifically to the deformation behaviour of the vertical elements (i.e. columns and walls); especially in the construction stage, when the load increases floor by floor. In fact, a realistic estimation of the vertical deformations is very important not only for the detailed design of the load-bearing components and their connections, but also, for general serviceability, e.g. of the facade elements. In the context of timber-hybrid buildings, an important question that arises is that of the deformation interaction between RC cores and timber columns. Since both construction materials have a different stiffness, a shift in vertical deformations can be expected. In fact, the typical modulus of elasticity of timber parallel to grain direction is

---

approximately three times lower than the typical modulus of elasticity of concrete in compression. In addition, both materials also possess a different shrinkage and creep behavior as a function of time.

For buildings such as *Arbo* the construction phase is typically lasting several weeks to months. Therefore, the influence of the often full weathering conditions can play an important role on the long-term deformation behavior of the vertical elements. The decisive factor is the interaction of the timber component's equilibrium moisture content (MC) and the specific moisture diffusion in the material with its mechanical behavior. Fluctuations in air humidity and temperature, both affecting the component's MC, can therefore have a considerable influence on their deformation. In the case of *Arbo*, beech laminated

veneer lumber (LVL) [11] and spruce glued laminated timber (GLT) were used for the columns. Although such engineered wood materials generally offer improved homogeneity and dimensional stability compared to solid wood, properties such as the complex time- and moisture-dependent mechanical behaviour are retained. Therefore, it is of interest for the design and engineering of tall timber buildings to being able to predict this type of deformation accurately. However, existing design guidelines do not cover this topic yet or give simplified, often highly conservative approaches.

In this study, a combined experimental and modelling assessment of vertical deformations of the columns of the case-study object *Arbo* was conducted. Both the columns and the column-to-ceiling transition
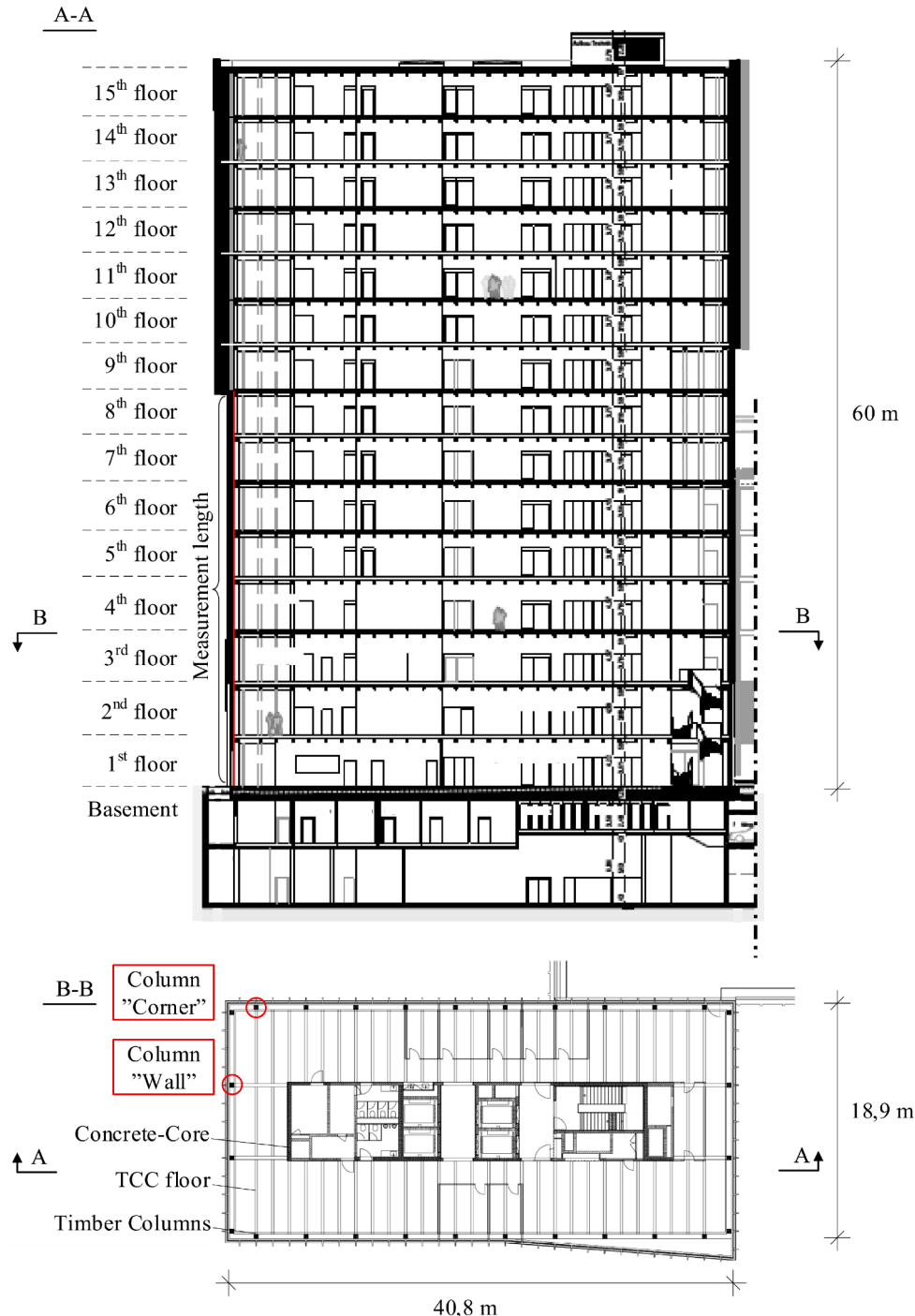

Fig. 1. Section of the high-rise building *Arbo* and floor plan of the 4th floor with labelling of examined column positions ("corner" and "wall").

components were monitored by fibre-optic strain measuring systems during a total time of 420 days after the start of the timber constructions. Hereby, both the full-weathering phase during the construction before installation of the facade elements and the sheltered, unheated phase after installation of the facade elements were included. The strains in the column elements were modelled using a simplified 1D rheological mechanical model for wood [12]. Such models include both the short and long-term deformation components of wood. Next to elasticity, time-dependent creep, moisture-dependent creep, and expansion caused by MC and temperature changes could be calculated. The use of such models in combination with an experimental monitoring study allowed to conduct a model verification for potential future use in practise-oriented design of tall timber buildings. Additionally, a research-oriented assessment of influence-cause relationships of the occurring deformations during the construction and service phase could be made. The insight based on the obtained measured and modelled data can contribute to a better understanding of the behavior of tall timber structures by the principle of design-led research and research-led design [13,14]. In this context in particular, it is of relevance to provide practising engineers with simple and straightforward calculation models that are verified by long-term monitoring studies.

2. Case-study object: tall timber-hybrid building Arbo

The building *Arbo* (Fig. 1) is Switzerland's second tall timber building and is located on the *Suurstoffi Areal* in the municipality of Risch-Rotkreuz in the canton of Zug. It is a 15-storey office building with canteen and library used by the Lucerne university of applied sciences and arts. It is 60 m high and was realized as a timber-hybrid construction. The construction started in 2017, the timber construction work started in May 2018 and the building was completed in November 2019. The client was *Zug Estates AG*, the architects *Manetsch Meyer Architekten AG* and *Büro Konstrukt AG, Lucerne*, and *Pirmin Jung Ingenieure AG* were responsible for the planning of the timber construction. The timber construction was carried out by the company *Erne AG Holzbau*.

The building *Arbo* consists of a RC core, stabilizing the structure, and a timber skeleton, supporting the structure. Unlike in the case of the *Brock Commons Tallwood House*, where the RC cores were entirely completed before the timber structure, the RC construction of *Arbo* was erected with a climbing formwork in stages ahead of the timber construction (Fig. 2). The RC core covers the staircase and provides horizontal bracing for the building (see also Fig. 1). The supporting timber structure in skeleton construction consists of columns assembled of softwood GLT and beech LVL, and of intercepting beams and ceilings in timber-concrete composite (TCC) construction. All components of the timber construction as well as the ceiling TCC elements were pre-fabricated in the factory and assembled on site.

Fig. 2. View of the building Arbo during construction with already completed concrete core and subsequent timber construction.

The building possesses different types of columns that possess themselves different types of cross-sections depending on the floor number. In this study, two column positions covering eight storeys are monitored and analyzed. Namely, column positions "wall" and "corner", see Fig. 1. The different cross-section layup follows the different required load-carrying capacity. The hybrid columns with a core of beech LVL (GL70 [11]) and surrounding sheathing of 20 mm softwood GLT (GL28h [15]) at the position "wall" are designed for a high load-carrying capacity. The columns at the position "corner" have a pure softwood GLT (GL28h [15]) cross-section and are designed for moderate load-carrying capacity. The specific column layup and dimensions at the two positions are shown in Table 1.

3. Materials and methods

3.1. Monitoring

3.1.1. Measuring system

Fibre optic sensors were used to measure the strain in the building components, which allow a high-resolution, continuous strain measurement along the timber columns. This technology is well established in monitoring deformations of timber elements [16–18]. A detailed description of the measurement technology can be found in [19]. The applied longitudinally distributed fibre optic sensor technology is based on the principle of spontaneous Rayleigh back-scatter along a glass fibre (optical back-scatter reflectometer). This allows strain measurement with a high spatial resolution along the sensor (10–20 mm) and a high accuracy ($\approx 5 - 10 \ \mu\varepsilon$) in each measurement section over a maximum distance of approx. 70 m. The respective columns positions "corner" and "wall" (see in Fig. 1) were equipped with both a strain sensor and a temperature sensor over a length covering 8 storeys from the floor on the ground level 1st floor to the ceiling of the 8th floor. The sensors are special strain sensing and temperature sensing fibre optic cables with coating made by Solifos AG. The diameter of the coated cables is 1.0 mm. A LUNA Optical Backscatter Reflectometer OBR [20] was used for the measurements and recording of the data. This device measures the wavelength shift of a laser due to reflected Rayleigh backscatter, which are dependent on the strain and temperature in the cable. The temperature sensors served to compensate for the temperature-related

Table 1
Structure of the column cross-sections of the different types of columns in the monitored storeys (Source: Pirmin Jung AG).

Storey	Position "wall"	Position "corner"
1st - 4th	Beech LVL 320/360mm / Softwood 20mm	GL28h 360/400mm
5th - 8th	Beech LVL 320/340mm / Softwood 20mm	GL28h 360/380mm

influences in the measurements of the strain sensors. The measurements as well as the compensation were carried out by the company *Marmota Engineering AG*.

3.1.2. Installation procedure of sensor cables

The instrumentation of the columns as well as the installation and splicing of the sensor cables was done in two steps. In a first step in factory, the two fibre optic sensor cables for strain and for temperature measurement were placed side by side in a 12 mm wide and 33 mm deep groove milled into the timber. The strain sensors were slightly pre-tensioned and glued in place with epoxy resin along the entire columns length except at two notches at the lower and upper end of the columns. The pre-tensioning was performed by pulling the fibre optic cable by hand. It ensures that the cable remains in an elongated state even when exposed to compression in the columns. The excess sensor lengths for the later splicing (lower end 1 m and upper end 1.2 m) were rolled up, stored in the notches and protected for transport. After instrumentation of the columns, the grooves were closed by wooden strips over the entire length of the glued-in sensors for protection for transport to the construction site and installation. In the second step, after moving the columns on site, the ends of two sensor cables of two adjacent columns were spliced together across the floor slab. After splicing, the cables were pre-tensioned and fixed across the floor slab. The remaining excess length of both cables was rolled up and placed in the notch at the foot of the upper column (Fig. 3). To protect the exposed sensors from the weather and ongoing work on the site, the notch in the concrete transition and at the head of the lower column and the foot of the upper column was then covered with protective adhesive tape. In the

course of the instrumentation some sensor cables were damaged and repair was not always possible.

3.2. Measurement stages

The erection of the columns with the sensor cables installed was carried out in the period from June 7th to August 27th, 2018. A baseline measurement of the first section of the sensor cables was carried out on June 7th, 2018, after the first column was erected. For each further piece of spliced sensor cable, a new baseline measurement was carried out. An overview of the actual measurements (following the baseline measurements) performed can be found in Table 2.

During the construction process damages on the sensor cables occurred. That is why not for all times of measurements results could be gained over the entire measurement length. The sensor cable at the measuring position "corner" was damaged above the 5th storey at measurement No. 6 and 7. The sensor cable at the measuring position

Table 2
Date of measurements and height of the timber structure.

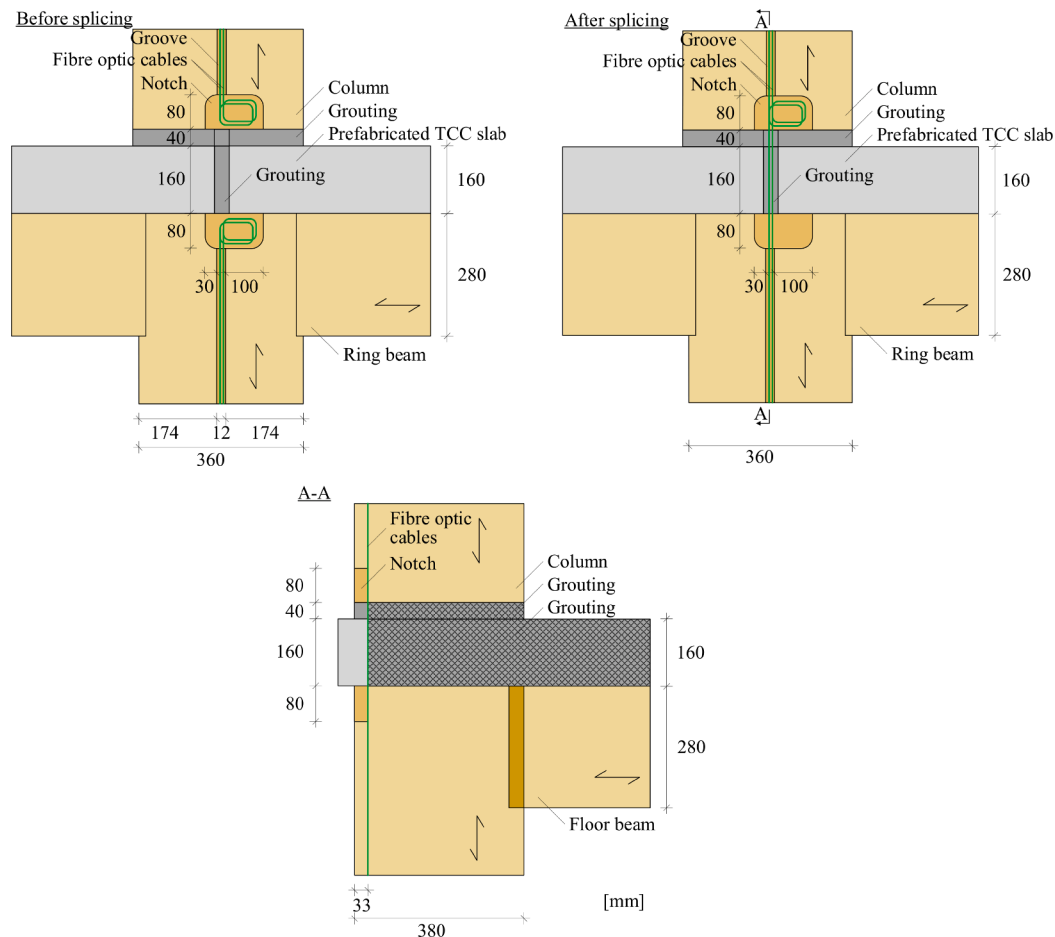| Measurement No.	Date	Construction progress timber
1	14.06.2018	2nd storey
2	03.07.2018	4th storey
3	30.07.2018	7th storey
4	27.08.2018	9th storey
5	08.01.2019	15th storey
6	03.04.2019	15th storey
7	15.07.2019	15th storey

Fig. 3. Detail of cable installation along column and ceiling transition: Front view before and after splicing, and cross-section; units in mm (adapted from ERNE AG Holzbau).

"wall" was not accessible in the final measurement No. 7.

The construction progress of the building as summarized in Table 2 can be converted into the relative ballast of the number of storeys acting on the columns of each storey as shown in Fig. 4. It can be seen that during the first 4 measurements (progress until 9th storey) the load in the columns increases approximately linearly. The loading in the upper storeys (no strain measurements during construction of 10th to 14th storey) follows the same trend. During the last 3 measurements over a seven month period after completion of the 15th storey, the load does not increase due to additional floors, but due to further permanent installations such as the raised floors and the technical building services. The subsequent installation of the facade elements followed at intervals of about 2–4 weeks after completion of the timber construction on the respective floor.

3.3. Modelling

3.3.1. Material model for timber columns

The theoretical background and calculation models for the deformation behaviour of the considered timber elements, along with measurement and calculation results of the neighbouring *S22* building, are described in detail in [21,6]. In the following paragraphs, the relevant modelling methods and parameters for the building *Arbo* are concisely summarized. The work of Becker [22], Hartnack [12], and Ranz [23] served as the theoretical basis for the modelling of the rheological material behaviour of the timber columns. Following their approach, it is assumed that the different influences on the long-term behaviour can be determined separately. This approach follows the assumption of the infinitesimal strain theory and the Boltzmann superposition principle. Hereby, the total strain (ε_{tot}) of the system is formulated as the sum of the individual strains of single serially-connected rheological elements as follows:

$$\varepsilon_{tot} = \varepsilon_{el} + \varepsilon_{vs} + \varepsilon_{ms} + \varepsilon_{sw} + \varepsilon_T \tag{1}$$

with the elastic strain ε_{el}, the strain from the visco-elastic deformation component ε_{vs}, the strains from the mechano-sorptive part ε_{ms}, the swelling and shrinkage strain ε_{sw}, and the strain due to temperature-induced expansion ε_T. The elastic strains at time t are calculated in analogy to a Hooke's spring element in dependence of the applied stress over time $\sigma(t)$ as

$$\varepsilon_{el}\left(t\right) = \frac{\sigma(t)}{E_0} \tag{2}$$

where E_0 represents the elastic stiffness of the timber column in grain direction. The visco-elastic strains at time t can be calculated following the solution of the constitutive differential equation of a series of four coupled Kelvin-Voigt rheological elements:

$$\varepsilon_{vs}\left(t\right) = \sigma_0 \sum_{k=1}^{4} \frac{\varphi_k}{E_0}\left(1 - e^{\frac{t}{\tau_k}}\right) + \sum_{i=1}^{n} \Delta\sigma_i\left[\sum_{k=1}^{4} \frac{\varphi_k}{E_0}\left(1 - e^{\frac{t-\tau_k}{\tau_k}}\right)\right]. \tag{3}$$

Hereby, φ_i are the creep factors and τ_i are the characteristic retardation times associated with each Kelvin-Voigt element i. The mechano-sorptive strain component is calculated as

$$\varepsilon_{ms}\left(t\right) = \frac{\sigma(t)}{E_{ms}} e^{-\frac{u(t)}{\Delta u_{max}}}, \tag{4}$$

where variable $u(t)$ designs the average MC of the timber column at time t, and $\Delta u_{max} = u_{max} - u_{min}$ is the maximum difference in MC that the column has experienced since time $t = 0$. E_{ms} is a material parameter related to the stiffness of the (single) mechano-sorptive Kelvin-Voigt element. The relative changes in length of the columns due to changes in MC, related to changes of the surrounding climate (relative humidity and temperature), can be calculated as follows:

$$\varepsilon_{sw}(t) = \overline{\alpha_L}\Delta u(t) \tag{5}$$

with $\Delta u(t)$ being the difference in MC between time t and $t = 0$. In order to compensate for the total deformation scenario, the adapted differential swelling coefficient $\overline{\alpha_L}$ can be calculated from the original differential swelling coefficient α_L with

$$\overline{\alpha_L} = \begin{cases} \alpha_L(1 - 180\varepsilon_{tot}) & \text{for } \varepsilon_{tot} \leqslant 0 \\ \alpha_L e^{(-180\varepsilon_{tot})} & \text{for } \varepsilon_{tot} > 0. \end{cases} \tag{6}$$

Finally, the relative length changes in as a function of changes in temperature (ΔT) are calculated as

$$\varepsilon_T(t) = \alpha_T\Delta T(t), \tag{7}$$

where α_T is the temperature expansion coefficient of the timber column.

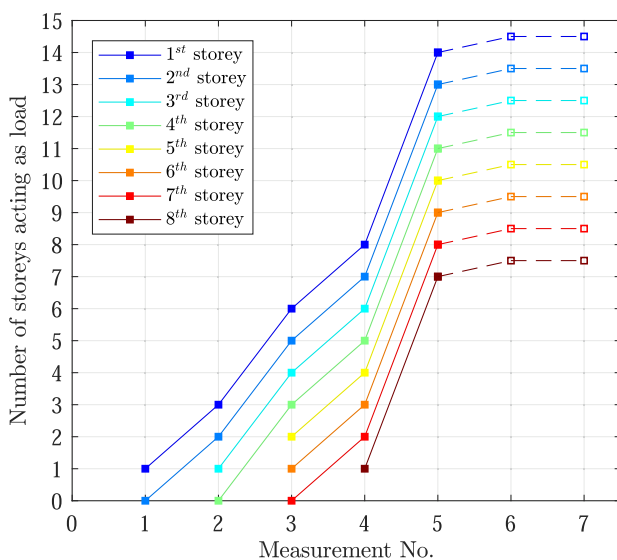#### 3.3.2. Model input parameters and procedure

The equations above were used to calculate the vertical deformations of both column positions "wall" and "corner" on the ground floor level (also denoted as 1st storey). The strains were calculated in a one-dimensional simplified manner along the column vertical directions (timber grain direction) for calculating the total vertical deformations along the height of a single column. The used geometric and elastic stiffness parameters (mean values according to [15,11]) of the two columns are summarized in Table 3. And for both columns, the parameters used in order to calculate the visco-elastic strains are summarized in Table 4. The parameter E_{ms} for the mechano-sportive strain component was calculated as

$$E_{ms} = \frac{\frac{E_0}{\alpha_L} \cdot 1.25 \cdot 10^{-3}}{\Delta u_{max}}. \tag{8}$$

Fig. 4. Increase of the load on measuring positions due to the number of floors above (relative ballast of the number of storeys acting on the columns of each storey) according to measurements in function of construction progress (Table 2).

Table 3
Geometric and elastic parameters used to model the timber columns.

Parameter	Column "wall"	Column "corner"
Height	3'800 mm	3'800 mm
Cross-section	360 × 400 mm	360 × 400 mm
E_0	16'800 MPa	12'600 MPa

Table 4

Creep factors and characteristic retardation times for calculation of visco-elastic strains by means of a chain with 4 Kelvin-elements following Becker [22].

Element	Creep factor φ_i [–]	Retardation time τ_i [h]
1	0.08	15
2	0.08	400
3	0.22	4'000
4	0.22	28'000

Furthermore, it was assumed that the timber columns possess coefficients of expansion in grain direction of $\alpha_L = 0.007\%/\%$ [24] for moisture and $\alpha_T = 5 \cdot 10^{-6} K^{-1}$ for temperature [25,26].

The deformations of the timber columns were determined incrementally throughout the time period of the monitoring measurements. The calculation increment size followed the increment size necessary for the calculation of the MC at time t described below in Section 3.3.3. However the load applied over time followed Table 2 and Fig. 4. The columns at the positions "wall" and "corner" carry different amounts of permanent loads dependent, amongst others, on the different influence areas of the load distribution from the slabs and the different lengths of the attached facade elements. The following permanent loads were used in the model for the loading of the columns:

- Dead weight of the columns made of beech LVL and softwood GLT.
- Total floor load of the TCC slabs was 4.2 kN/m^2. Influence areas of approx. 9 m^2 for the position "corner" and 13 m^2 for the position "wall".
- The weight of the element facade was set as 1 kN/m^2 facade surface area according to the usage agreement.

3.3.3. Moisture content calculation

For the calculation of the mechano-sorptive creep as well as the swelling and shrinkage components, an average wood MC in the entire cross-section of the column was assumed. This value was determined by averaging the calculated distribution at time t in the cross-section. The moisture distribution over time was calculated using a one-dimensional diffusion Eq. (2nd Fick's law) for the timber elements parallel to the grain direction and possessing a diffusion coefficient D:

$$\frac{\partial u}{\partial t} = D \frac{\partial^2 u}{\partial x^2}. \tag{9}$$

Using the Finite Difference method, the above equation can be reformulated to an incremental form with respect to the MC u:

$$\frac{u_j^{i+1} - u_j^i}{\Delta t} = D \frac{u_{j+1}^i - 2u_j^i + u_{j-1}^i}{(\Delta x)^2}. \tag{10}$$

Hereby, superscripts i refer to a time step and subscripts j refer to co-ordinates in the cross-section of the timber columns. For the diffusion coefficient, the value $D = 0.5 \cdot e^{4.0u} \, mm^2/h$ was used. Differences of the diffusion coefficient in absorption and desorption was neglected since it shows only a minor impact in the case study. The starting MC was assumed to be $u_j^0 = u_0 = 7\%$ for the calculations of both columns "wall" and "corner", according to manufacturer specifications. The boundary condition of the timber column surface, following Babiak [27] and Becker [22], describing the interaction of surface MC to surrounding climate, was used as follows:

$$u_0^{i+1} = \left(u_{RH} - u_0^i\right)\left(1 - e^{-\beta t}\right), \tag{11}$$

where 0.03 1/h was used as the value of the surface emission coefficient β. The equilibrium MC u_{RH} was calculated in dependence of the relative air humidity φ_r at the columns following Kollmann [28] as

$$u_{RH} = 0.108\varphi_r^{0.64} + 0.202 e^{-\frac{1}{2}(2.75(\varphi_r - 1) - 1)^2} + 0.10 e^{-\frac{1}{2}(21.0(\varphi_r - 1) - 1)^2}. \tag{12}$$

Finally, in the middle of the cross-section, a symmetry boundary condition ($u_{j-1}^i = u_{j+1}^i$) was used. Therefore, the wood MC at increment $i+1$ was determined as

$$u_j^{i+1} = 2D\left(u_{j-1}^i - u_j^i\right). \tag{13}$$

Using the above equations and respecting the Neumann and Courant-Friedrichs-Lewy stability criteria, the moisture distribution in the timber column cross-sections were incrementally determined over the whole monitoring period of the columns as function of φ_r. The relative air humidity variation $\varphi_r(t)$ was modelled as a sinusoidal function, which was determined using a best fitting based on in situ meteorological data retrieved over the time period of the construction phase [21]. Temperature variations were also modelled as fitted sine functions.
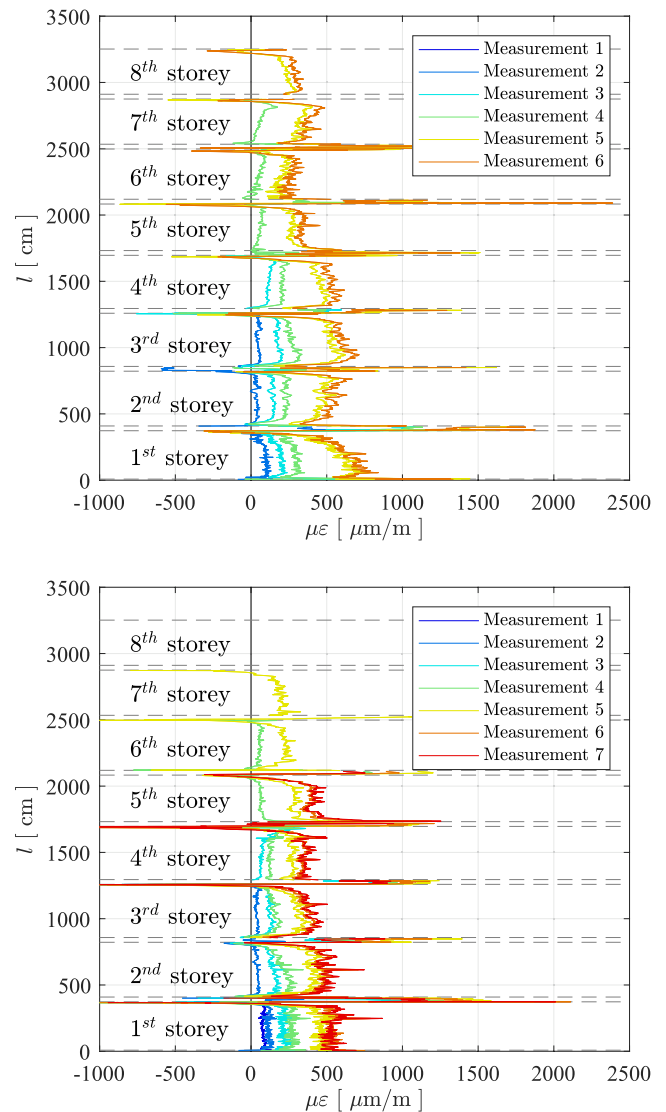
Fig. 5. Strain development along the column positions "wall" (top) and "corner" (bottom). Measurement data is expressed in micro-strain ($10^{-4}\%$) and interval length between the individual measurement points is 1.02 cm. Positive measured values correspond to a compression of the elements.

4. Results and discussion

4.1. Measurement results

Fig. 5 shows the cumulative strain changes at the time of the single measurements with increasing construction progress along the respective measurement length along the building height. The strains incorporate the temperature compensation. The increase of the strains due to increasing load during the course of the construction progress is clearly reflected. The column "wall" shows higher strains than the column "corner", which can be explained only partly by the higher loads acting on the column "wall". The latter is mainly beech LVL, which is more stiff than the spruce GLT from the column "corner". For both columns, a pronounced variation of the strains along the measurement length for each individual measurement can be observed. Segments of higher strains and strain peaks can be identified, which are located in the regions of the connections of the columns with the concrete ceilings and the transition of the cables in these regions (cf. Fig. 3). However, along the central segments of the columns a relatively even strain distribution can be observed.

The strains in the central segment of the columns at a distance of 58 cm from the base of the column and up to 58 cm before the head of the column were averaged for each storey for comparison. In Fig. 6 these strains are plotted for all measurements over the course of the construction progress and the building height for the columns at positions "wall" and "corner". The steady increase of strain in function of the construction progress can be observed again. However, a storey-wise shift in average strain in function of storeys above acting as load can only be partly observed. The shift is inconsistent and does not show a clear trend as some values, at both column positions, break the pattern of storey number (the lower the storey, the higher the strain). This may be due to the choice of averaging segment length or higher loads than expected during baseline calibration.

While the strains in the column mid-segments were relatively uniform, it can also be seen in Fig. 5 that the strains in the transitions through the ceilings are highly variable. For comparison, only the strains in the region of the prefabricated TCC slabs were averaged and are shown in Fig. 7 for both column positions. The average strains in the ceiling transitions are higher by up to a factor of 2 as compared to the average strains in the columns. However, as in Fig. 5, the data is highly inconsistent and no obvious trends may be observed.

The absolute deformations of the different elements along the measurement length can be calculated from the measured strains and the interval length between the individual measuring points. Fig. 8 shows the absolute deformations of the different columns and ceiling transitions for the positions "wall" and "corner". On the one hand it can be seen that the absolute deformations in the columns of the measuring position "wall" are larger than at the measuring position "corner". At the positions "wall", the columns in the 1st-4th storey all show a similar deformation between values of 2.2 and 2.5 mm at the 6th measurement. Storeys 5 to 8 display values between 1 and 1.5 mm. At the position "corner", storeys 1 and 2 reach around 2 mm and storeys 3 to 5 reach around 1.5 mm. On the other hand, the absolute deformations of the ceiling transitions are clearly smaller, reaching maximum deformations of around 0.25 mm in all cases. Despite the larger strains, this is explained by the fact that the length of the ceiling transitions is clearly smaller compared to the column lengths.

In summary, the columns with higher loading reached higher strains but the highest strains could be measured in the ceiling transition zones. However, the highest component deformations were measured in the columns, where values up to 2.5 mm are reported per storey and per column after an approximate duration of the monitoring of one year and one month. This data can be deemed reliable considering the general strain progression shown in Fig. 5 and the measurement precision of the sensors ($\approx 5-10 \ \mu\varepsilon$).

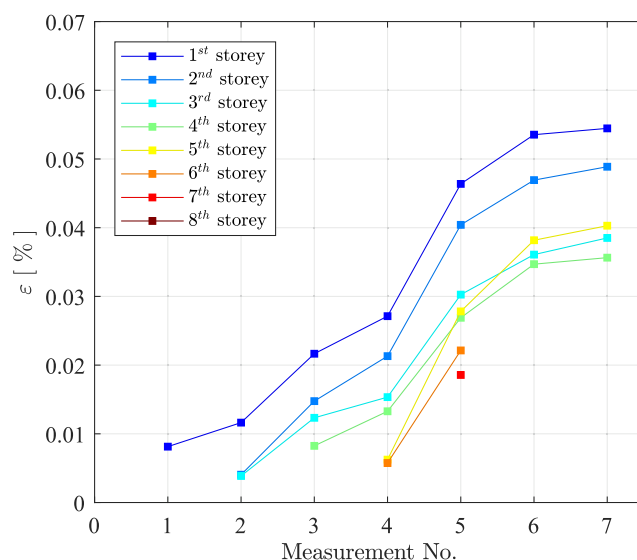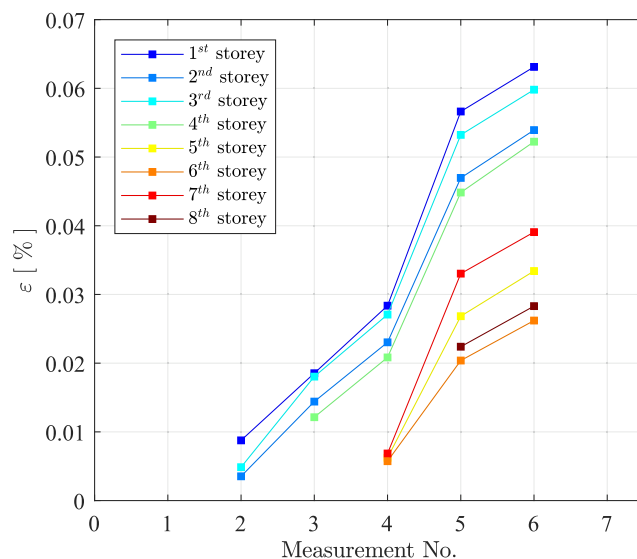The total measured deformation is approx. 8 mm on top of the 5th

Fig. 6. Average strains over the measurement length in the columns at the measuring position "wall" (top) and the measuring position "corner" (bottom).

storey at the position "corner" (at measurement No. 7) and approx. 14 mm on top of the 8th storey at the position "wall" (at measurement No. 6). It should be considered that this deformation does not consider the initial settlement from assembly and that the connection points are not properly covered due to discontinuities in these regions.

4.2. Comparison of measured and predicted deformations

Fig. 9 shows the modelled and measured deformations in the highest loaded columns in the ground floor (1st storey) for positions "wall" (top) and "corner" (bottom) over a length of 3.80 m. The stair-like course of the modelled deformations represents the increase in elastic and total deformation due to the increasing load during the construction progress of the first 180 days. The load increases mainly due to the addition of further storeys but also due to the installation of the facade elements. It can be recognized that the total model deformations reach 3 mm for the position "wall" and 2.5 mm for the position "corner". From the total deformations at $t = 420$ days, approximately 25% can be attributed to visco-elastic creep and about 8% to mechano-sorptive creep. Due to the small seasonal changes in humidity and the long diffusion paths in the columns, the swelling and shrinkage (as well as the mechano-sorption)
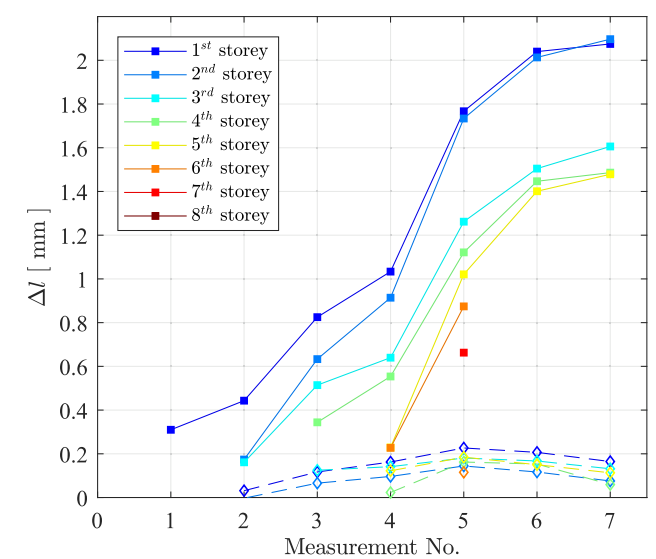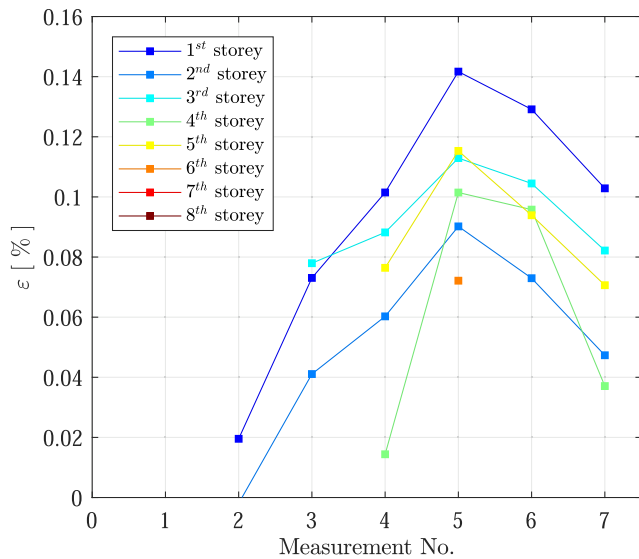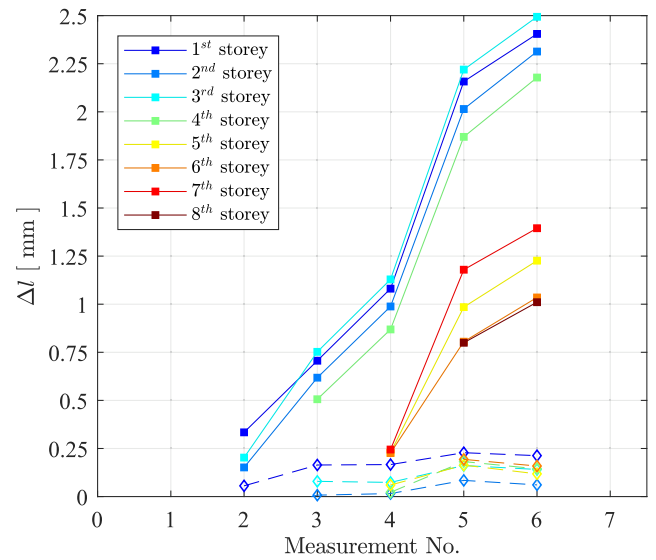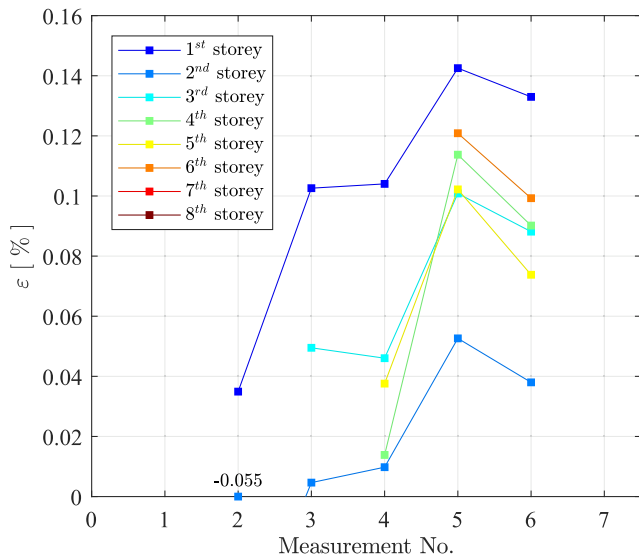
Fig. 7. Average strains over the ceiling transitions at the measuring position "wall" (top) and the measuring position "corner" (bottom).

Fig. 8. Absolute deformations in the columns (solid lines) and ceiling transitions (dashed lines) in the measuring positions "wall" (top) and "corner" (bottom).

remained rather low and only started after 120 and 210 days after the start of the construction. In fact, a maximal average change of about 1.5% wood MC was modelled from the diffusion analysis. The authors recommend for future studies to install moisture sensors and monitor the MC in the structure in order to make a better prediction of the moisture dependent deformations.

During the construction phase ($t = 0$ to $t = 180$ days), it can be seen that the linear elastic deformations alone predict the measured deformations accurately. Therefore, it can be concluded that long-term deformation play only a marginal importance during the time when the building is still under construction. However, at $t = 420$ days it can clearly be recognized that a third of the total deformations are caused by the long-term components and that those components still show a trend of increasing at this time. In fact, the mechano-sorptive component will be steadily increasing as long as the seasonal changes in relative humidity happen, and i.e., for the rest of the structure's lifetime. In contrast, the visco-elastic portion will show an asymptotic behavior and stop increasing.

The validity of the chosen modelling approach for predicting the long-term column deformations with a rheological model can in general be confirmed based on the two columns investigated in the ground floor

(Fig. 9). The experimental data clearly shows that the calculated deformations agree well with the measured deformations both during the construction phase and during a long-term phase of approximately 240 days after the end of the construction phase. However, while at the position "corner" the column is made of pure softwood GLT and the parameters of the rheological model for visco-elasticity and mechano-sorption taken from literature therefore correspond to reality, the column at the position "wall" is a hybrid mainly made of beech LVL. For the latter material, the same parameters as for spruce GLT were used in order to model the visco-elastic and the mechano-sorptive components due to lack of specific parameters for beech and particularly beech LVL. In order to enable a more precise modelling of the position "wall", such parameters would be necessary for beech LVL, which is a relatively new construction material in Europe [11]. While multiple studies analyzed its potential for application in timber engineering, e.g. [29–31], or more recently, its physical interaction with moisture [32], there are hardly any creep and long-term tests with this material due to the relatively short time since its market launch.
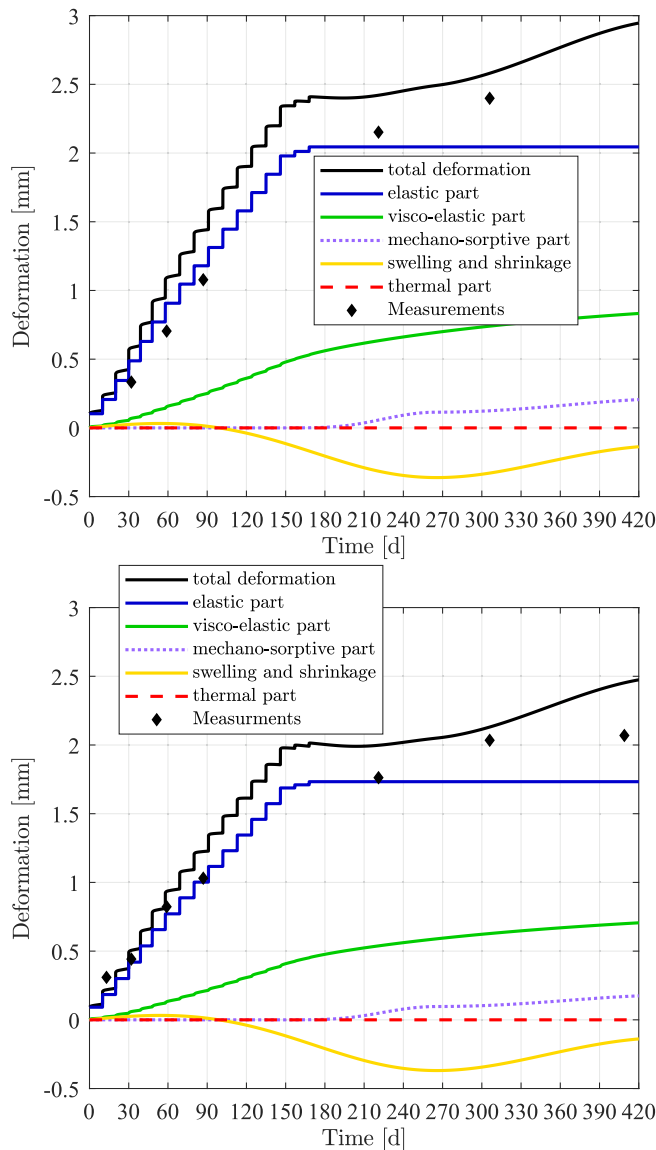
Fig. 9. Comparison of the modelled and measured deformations in the measuring position column "wall" (top) and "corner" (bottom) over a length of 3.80 m on the ground floor.

4.3. Modelling temperature expansion

Temperature and relative air humidity, as well as temperature and wood MC, are always physically coupled with each other so that these effects can hardly be separated and characterized independently with respect to deformations [33]. In addition, temperature-dependent expansions, even in the direction of the wood fibres, are always about one order of magnitude smaller than those caused by MC changes. For these reasons, temperature expansions are usually neglected when modelling wood or timber products. However, since the columns under consideration in this study run over entire floors, and thus the calculated length to which the strains refer is large, it was decided to take the strains due to temperature into account. Nonetheless, Fig. 9 clearly shows that the temperature expansions can be neglected also in the case of long timber elements.

4.4. Limitations of the used model

Although the used model was able to predict both the short and the long term deformations within an acceptable range of accuracy in terms

of design in timber engineering, it is of simple nature and some limitations need to be mentioned in order to set boundaries for its application. Effects or parameters which are not considered in the model can be summarized as follows:

- The anisotropy of the timber material was neglected and both the deformation resulting from the vertical load and the moisture diffusion in the transverse direction of the column were calculated in a simplified (one-dimensional) way. The model and calculations need to be adapted in cases where the transverse behavior is relevant.
- The elastic stiffness moduli of the columns (E_0) were assumed to be constant. In reality they are variable and depending on the actual wood MC [34]. This aspect is highly relevant for structures where large changes in MC are to be expected.
- The assumption of the linear visco-elasticity of wood is only valid under certain load limits. Becker [22] and Ranz [23] give a utilization factor of approx. 40 to 80% of the short term strength as the limit for the assumption of linear visco-elasticity. The model thus neither considers independent plastic deformations or irreversible visco-elastic and mechano-sorptive components.
- The modelled stresses were calculated from best estimates of the loads from the different construction stages. Therefore they do possibly not reflect the real acting stresses on the individual modelled columns.

The simple 1D calculation model used in this study was explicitly chosen with respect to the limiting factors mentioned above. In fact, columns represent simple single-part systems, for which the limitations do not raise relevant objections. However, in cases of more complex geometry, or cases requiring complex analyses, the use of more advanced numerical methods, such as e.g. the Finite Element (FE) method, is suggested. Implementations of rheological models for wood into commercial FE frameworks are already available [35]. Such models allow 3D investigations of coupled moisture diffusion and long-term mechanical analyses of arbitrary timber elements. E.g., analysis of stresses and strains or cracks induced by moisture gradients upon drying [36,37]. The drawback is their general complexity, which renders them inadequate for use in practical engineering for the design of timber structures.

4.5. Engineering implications

For the purpose of engineering verification, e.g. of serviceability, the deformations of timber components are calculated with the elasticity theory. However, if timber components are stressed over a longer period of time, creep deformations need to be taken into account. In Swiss SIA standards for structural timber design [38,26], creep deformations, as a result of permanent actions and the quasi-permanent portions of variable actions, may be determined approximately as $1 + \varphi$ times the corresponding elastic deformations. In Eurocode 5 [39] the corresponding value is k_{def}, which reduces stiffness values by dividing by $1 + k_{def}$. For the case-study object *Arbo*, the corresponding design values for moisture (SIA) or service (Eurocode) class 1, are $\varphi = k_{def} = 0.6$. By taking a look at the highest stressed columns in Fig. 9, it can be seen that the long-term deformations, as measured at approximately 300 days (position "wall") and 420 days (position "corner") result in lower values. At the position "wall" $1 + \varphi = 1 + k_{def} \approx 1.25$ (2.5 mm divided by 2.0 mm) for $t = 300$ days, and at the position "corner" $1 + \varphi = 1 + k_{def} \approx 1.20$ (2.1 mm divided by 1.75 mm) for $t = 420$ days. Therefore, it can be said that both standards list conservative values for highly stressed timber columns of tall timber buildings, as verified by the presented case-study over a 420 day period.

On the one hand, the combination of time and moisture-dependent creep, where the latter part is continuously increasing due to climate

variations in service, may lead to deformations potentially exceeding the guideline values over several decades. Whether or not this scenario can happen is especially unknown for new materials such as beech LVL, where as stated above, important material parameters for long-term calculations are still missing. On the other hand, future monitoring and modelling studies such as the one shown in this study, provided the modelling parameters are adequate (cf. beech LVL) and that the model can be verified, would potentially allow for less conservative design of the serviceability limit states in the future. Such considerations could be relevant, e.g. in the case of tall timber-hybrid buildings, with respect to estimating and designing long-term deformation differences between the timber elements and the RC cores.

5. Conclusions

In the highly stressed columns of the tall timber building *Arbo*, an increase in deformation with increasing load could be reliably measured during construction and initial service lifetime by using fibre optic sensors. Model calculations using a rheological model for the timber elements show a good agreement of the long-term deformation increase and can confirm the level of deformations during the construction state. This was also true in the case of the columns made from the novel product beech LVL. Furthermore, the measured deformations in the highly stressed columns at the time of the measurements are below the theoretical deformations which can be determined with the factor $k_{def} = 0.6$ according to Eurocode 5. However, for long-term periods over multiple decades the service climate variation could potentially cause an unknown amount of deformation due to moisture-dependent creep (mechano-sorptive effect). Especially in view of engineering assessment in this regard, further material properties, e.g. for beech LVL, and further long-term monitoring studies are needed.

Declaration of Competing Interest

The authors declare that they have no known competing financial interests or personal relationships that could have appeared to influence the work reported in this paper.

Acknowledgement

References

[1] Foster RM, Reynolds TPS, Ramage MH. Proposal for defining a tall timber building. J Struct Eng 2016;142(12):02516001. https://doi.org/10.1061/(ASCE)ST.1943-541X.0001615.

[2] Cornwall W. Tall timber. Science 2016;353(6306):1354–6. https://doi.org/10.1126/science.353.6306.1354.

[3] Skullestad JL, Bohne RA, Lohne J. High-rise timber buildings as a climate change mitigation measure – a comparative LCA of Structural System Alternatives. Energy Proc 2016;96: 112–123, sustainable Built Environment Tallinn and Helsinki Conference SBE16. doi:10.1016/j.egypro.2016.09.112.

[4] VKF, Brandschutzvorschriften, VKF – Vereinigung Kantonaler Feuerversicherungen, Bern, Switzerland, 2015.

[5] Lignum, Hochhaus, holzbulletin 135, Report, Lignum Holzwirtschaft Schweiz, Zurich, Switzerland; 2020.

[6] Jockwer R, Fröhlich R, Wydler J, Voulpiotis K, Schabel J, Frangi A. Deformation behaviour of highly loaded elements in tall timber buildings. In: Proceedings of the World Conference on Timber Engineering (WCTE 2018), WCTE, Seoul, Korea; 2018.

[7] Kuzmanovska I, Gasparri E, Tapias Monne D, Aitchison M. Tall timber buildings: Emerging trends and typologies. In: Proceedings of the World Conference on Timber Engineering (WCTE 2018), WCTE, Seoul, Korea; 2018.

[8] Forestry Innovation Investment, naturally:wood, Case study: Brock commons – design & preconstruction overview, Tech. rep., https://www.naturallywood.com/resources/brock-commons-design-preconstruction-overview (URL retrieved on 10.08.2020); 2016.

[9] Fast P, Gafner B, Jackson R. Eighteen storey hybrid mass timber student residence at the University of British Columbia. Struct Eng Int 2017;27(1):44–8. https://doi.org/10.2749/101686617X14676303588553.

[10] Tannert T, Moudgil M. Structural design, approval, and monitoring of a UBC Tall Wood. Building 2017:541–7. https://doi.org/10.1061/9780784480410.045.

[11] Hassan J, Eisele M. Baubuche – der nachhaltige Hochleistungswerkstoff. Bautechnik 2015;92(1):40–5.

[12] Hartnack R. Langzeittragverhalten von druckbeanspruchten Bauteilen aus Holz. PhD Thesis. Weimar, Germany: Bauhaus-Universität; 2004.

[13] Smith I, Frangi A. Overview of design issues for tall timber buildings. Struct Eng Int 2008;18(2):141–7. https://doi.org/10.2749/101686608784218833.

[14] Ramage M, Foster R, Smith S, Flanagan K, Bakker R. Super tall timber: design research for the next generation of natural structure. J Architect 2017;22(1): 104–22. https://doi.org/10.1080/13602365.2016.1276094.

[15] CEN, EN 14080: Timber structures – Glued laminated timber and glued solid timber – Requirements, European Committee for Standardization CEN; 2013.

[16] Leyder C. Monitoring-based performance assessment of an innovative timber-hybrid building, Doctoral Thesis, ETH Zurich; 2018. doi:10.3929/ethz-b-000288684.

[17] Leyder C. Monitoring-based performance assessment of an innovative timber-hybrid building, Report, ETH Zurich, Zurich, Switzerland, iBK Bericht No. 503; 2019. doi:10.3929/ethz-b-000337054.

[18] Palma P, Steiger R. Structural health monitoring of timber structures – review of available methods and case studies. Constr Build Mater 2020;248:118528. https://doi.org/10.1016/j.conbuildmat.2020.118528.

[19] Iten M. Novel applications of distributed fiber-optic sensing in geotechnical engineering, Doctoral Thesis, ETH Zurich; 2011. doi:10.3929/ethz-a-6559858.

[20] LUNA, https://lunainc.com/ (URL retrieved on 17.09.2020); 2020.

[21] Fröhlich R, Wydler J. Hochhäuser aus Holz – Verformungsverhalten hochbeanspruchter Tragelemente, Master-Projektarbeit, ETHZ – Institut für Baustatik und Konstruktion, Zurich, Switzerland; 2017.

[22] Becker P. Modellierung des zeit-und feuchteabhängigen Materialverhaltens zur Untersuchung des Langzeittragverhaltens von Druckstäben aus Holz. Shaker: Berichte aus dem Bauwesen; 2002.

[23] Ranz T. Viskoelastisches Materialmodell für Holz: Experimente, Modellierung und Simulation, Fortschrittberichte VDI/ 18: Mechanik. Bruchmechanik: VDI-Verlag; 2009.

[24] Toratti T. Creep of timber beams in a variable environment, VTT; 1992.

[25] F.P. Laboratory, Wood handbook: Wood as an engineering material. General Technical Report FPL-GTR-190, U.S. Department of Agriculture, Forest Service, Forest Products Laboratory; 2010.

[26] SIA, Standard SIA 265/1 – Timber Structures – Supplementary Specifications, SIA Swiss Society of Engineers and Architects, Zurich, Switzerland; 2018.

[27] Babiak M. Is Fick`s law valid for the adsorption of water by wood? Wood Sci Technol 1995;29(3):227–9.

[28] Kollmann F. Zur Theorie der Sorption. Forschung auf dem Gebiet des Ingenieurwesens A 1963;29(2):33–41. https://doi.org/10.1007/BF02558925.

[29] Boccadoro L, Frangi A. Experimental analysis of the structural behavior of timber-concrete composite slabs made of beech-laminated veneer lumber. J Perform Constr Facil 2014;28(6):A4014006. https://doi.org/10.1061/(ASCE)CF.1943-5509.0000552.

[30] Dill-Langer G, Aicher S. Glulam composed of glued laminated veneer lumber made of beech wood: Superior performance in compression loading. In: Aicher S, Reinhardt H-W, Garrecht H, editors. Materials and Joints in Timber Structures. Netherlands, Dordrecht: Springer; 2014. p. 603–13.

[31] Kobel P, Frangi A, Steiger R. Timber trusses made of European beech LVL. In: Proceedings of the World conference on timber engineering (WCTE 2016), Vienna, Austria; 2016.

[32] Benthien JT, Riegler M, Engehausen N, Nopens M. Specific dimensional change behavior of laminated beech veneer lumber (baubuche) in terms of moisture absorption and desorption, Fibers 2020;8(7). doi:10.3390/fib8070047.

[33] Goli G, Becherini F, Di Tuccio MC, Bernardi A, Fioravanti M. Thermal expansion of wood at different equilibrium moisture contents. J Wood Sci 2019;65(1). https://doi.org/10.1186/s10086-019-1781-9.

[34] Gerhards C. Effect of moisture content and temperature on the mechanical properties of wood: an analysis of immediate effects. Wood Fiber Sci. 1982;14(1): 4–36.

[35] Hassani MM, Wittel FK, Hering S, Herrmann HJ. Rheological model for wood. Comput Methods Appl Mech Eng 2015;283:1032–60. https://doi.org/10.1016/j.cma.2014.10.031.

[36] Hassani MM, Wittel FK, Ammann S, Niemz P, Herrmann HJ. Moisture-induced damage evolution in laminated beech. Wood Sci Technol 2016;50(5):917–40. https://doi.org/10.1007/s00226-016-0821-5.

[37] Grönquist P, Wood D, Hassani MM, Wittel FK, Menges A, Rüggeberg M. Analysis of hygroscopic self-shaping wood at large scale for curved mass timber structures. Sci Adv 2019;5(9). https://doi.org/10.1126/sciadv.aax1311.

[38] SIA, Standard SIA 265 – Timber Structures, SIA Swiss Society of Engineers and Architects, Zurich, Switzerland; 2012.

[39] CEN, EN 1995-1-1: Eurocode 5: Design of timber structures – Part 1–1: General – Common rules and rules for buildings, European Committee for Standardization CEN, Bruxelles, Belgium; 2004.

[40] Jockwer R, Grönquist P, Frangi A. Verformungsverhalten von Holzstützen: Erkenntnisse aus dem Monitoring von zwei Holz-Hochhäusern, Report, ETH Zurich, Zurich, Switzerland, final Report of Project No. 2017.03, Wald- und Holzforschungsfonds WHFF; 2020.